Ahmed, H.; Punkki, J.

Methods for Assessing Concrete Segregation Due to Compaction

Published in:
Nordic Concrete Research

DOI:
10.2478/ncr-2023-0013

Published: 05/07/2024

Document Version
Publisher's PDF, also known as Version of record

sciendo	Nordic Concrete Federation
© Article authors. This is an open access article distributed under the Creative Commons Attribution-NonCommercial-NoDerivs licens. (http://creaticecommons.org/licenses/by.nc-nd/3.0/).	ISSN online 2545-2819 ISSN print 0800-6377
DOI: 10.2478/ncr-202023-0013	Received: Oct. 23, 2023 Revision received: Feb. 10, 2024 Accepted: Feb. 19, 2024

Methods for Assessing Concrete Segregation Due to Compaction

Hassan Ahmed
M.Sc.
Department of civil engineering, Aalto University
Rakentajanaukio 4 A, 02150 Espoo, Finland
e-mail: hassan.ahmed@aalto.fi

Jouni Punkki
Ph.D., Professor of practice
Department of civil engineering, Aalto University
Rakentajanaukio 4 A, 02150 Espoo, Finland
e-mail: jouni.punkki@aalto.fi

ABSTRACT

Segregation in concrete significantly affects its durability and structural integrity by introducing local variance in both the strength distribution and the modulus of elasticity within a structural element. Additionally, segregation can lead to durability complications, such as shrinkage induced cracking. Recent observations have identified such segregation issues in already existing structures, underscoring the importance of assessing segregation. In this study, we evaluate the extent of segregation in normally vibrated concrete specimens, which were subjected to different vibration durations and vibrated using either table or poker vibrators. The research introduces three segregation indices to assess this phenomenon. One index relies on the standard deviation of densities across multiple slices of each specimen, while the other two utilize Digital Image Processing (DIP) to analyse the distribution of aggregates in horizontal and vertical slices, respectively. High correlations were found between the density-based index and vibration time for both poker-vibrated and table-vibrated specimens. The DIP-based indices showed strong correlations with the density-based approach, offering quicker alternatives for assessing segregation. The study further proposes classification levels for segregation based on these methods and reveals the negative impact of increased air entrainment on segregation. These findings provide insights for optimizing concrete compaction processes and understanding segregation.

Key words: Concrete segregation, compaction, density distribution, aggregate distribution, digital image processing.

1. INTRODUCTION

Strength and durability are fundamental attributes of concrete, largely attained through a well-balanced distribution of its constituent materials [1,2]. This balance, however, can be compromised by segregation, where components of concrete, particularly coarse aggregates, air, or mortar, become unevenly distributed within the mixture [1–9]. Another form of segregation is bleeding, where water rises to the surface as heavier constituents sink under the force of gravity. Segregation in concrete can arise from either poor mix design [4] or improper placing and compaction [3,4,6–9]. Design-related factors include selecting a consistency unsuitable for the intended application, incorporating excessive amounts of large aggregates, or having a significant density difference among aggregates [4]. On the other hand, improper placing techniques, such as dropping concrete from a height or discharging it against an obstacle, can lead to segregation [3,4]. Most notably, over-compaction remains a primary cause for segregation in concrete [3,4,6–9].

Compaction is a critical process for Normally Vibrated Concrete (NVC) and it is carried out via vibration. The main objectives of compaction are to remove entrapped air from fresh concrete and to ensure the concrete fills moulds effectively [10,11]. Improper compaction can significantly affect the strength and durability of NVC. Under-compaction may leave between 5–20% entrapped air by volume in NVC, with the potential of this air being concentrated in certain parts, leading to a form of air segregation that reduces density and thereby compromising the strength and durability [11]. Conversely, over-compaction induces aggregate segregation, leading to large variations in densities that cause durability and strength issues [6,11]. Hence, the compaction process for NVC should aim to effectively expel entrapped air while minimizing the risk of segregation as much as possible [10].

Researchers employed different methods to estimate the level of segregation in NVC [6,9,12,13]. Some researchers analysed segregation in concrete by counting aggregates from vertically sawn sections [6,9,12]. Khayat and Guizani [12] divided these sections into multiple subsections, determining the percentage of aggregates larger than 5 mm within each. They then calculated a segregation index based on the sum of squares approach, where a higher index value indicates greater segregation. Conversely, Navaratte and Lopez [6] focused on the top and bottom subsections, estimating segregation through an index that considers the absolute difference between those subsections, normalized by their combined sum. Ojala et al. [9] adopted a similar approach but set a limit of 8 mm for aggregate size. Their segregation index was based on the percentage difference between the top and bottom parts. A common limitation of these methods is the reliance on manual counting of aggregates, which is labour-intensive and time-consuming.

Ojala et al. [9] also relied on density measurements to derive another segregation index. By drilling cores from the top and bottom sections of hardened concrete specimens and measuring their respective densities, they determined a segregation index based on the density difference between these cores. However, this approach, relying solely on two measurements, might not capture the full segregation profile of the specimen. Additionally, they [9] employed AC-impedance spectroscopy as a tool to identify the onset of segregation in fresh concrete during compaction. However, the authors designed this technique as a detection method and not to quantify the extent of segregation.

Safawi et al. [13] measured segregation in fresh highly flowable NVC using wet sieving, where they cast concrete into a form divided into five parts using metal slides. Subsequently, coarse aggregates larger than 5 mm from each section were isolated, washed, and weighed to determine their percentage by weight in relation to the total concrete. A segregation index was calculated as the normalized variance in the coarse aggregate concentration across different sections relative to the average concentration in the entire sample. However, this method cannot be applied to already existing structures or samples of hardened concrete.

While the emphasis of this article is on NVC, it is worth mentioning that segregation is not exclusive to NVC. Other concrete types are also prone to segregation, such as Light-Weight Aggregate Concrete (LWAC) and Self-Compacting Concrete (SCC). The former is susceptible to segregation due to the large difference in densities of its components [14], while the latter is prone to segregation because of the use of high dosages of superplasticizer and high cement paste contents among others [15].

Regarding LWAC, Solak et al. [7] and Barbosa et al. [16] utilized Digital Image Processing (DIP) techniques to propose segregation indices for LWAC. They based their assessment on the distribution of Lightweight Aggregates (LWA) in LWAC sections, using colour thresholding to generate binary masks that differentiate between LWA and cement paste. However, the aggregates used in both studies were all of almost one uniform colour, a condition that may not always be representative of the diverse colour range found in aggregates used in various concrete mixes. Additionally, Ke et al. [17] proposed a segregation index that relies on density measurements from the top and bottom portions of LWAC specimens. As previously mentioned, such approach does not consider the full segregation profile of a specimen.

n the context of SCC, Mesbah et al. [18], Nili et al. [19], and Yim et al. [15] introduced segregation indices based on electrical measurements to detect segregation in fresh SCC. These indices showed a good correlation with results derived from wet-sieving. However, as previously discussed, such methods are not suitable for evaluating segregation in existing structures. The mechanisms of segregation in LWAC and SCC differ from those in NVC. In LWAC, aggregates tend to float upwards, contrasting with the downward sinking observed in NVC [4]. Additionally, SCC, unlike NVC, does not require post-placement vibration due to its reliance on static stability to resist segregation [2]. Despite these differences, developing robust segregation indices for NVC is valuable, as they could be adapted to analyse segregation of LWAC and SCC.

In recent years, segregation of NVC has resurfaced as a problem in the Finnish concrete industry. This was investigated by Ojala et al. [20], who observed significant density variations in test structures, particularly in concretes with higher fluidity and air entrainment, indicating a pronounced risk of segregation. Similarly, the Federal Waterways Engineering and Research Institute in Germany (BAW) [21] reported recent several instances of severe segregation within lock chamber walls, identifiable through visual inspection and evident as a clear separation of aggregates from the mortar.

Given the lack of standardized methods for quantifying the degree of segregation, controlling this issue in the concrete industry remains a challenging task. Addressing this critical gap, this research aims to evaluate the extent of segregation based on density measurements for multiple concrete specimens vibrated by two different methods: table vibrator and poker vibrator. This study also offers a quantification of the levels of segregation for the studied concrete mix, which can be further extended to other mixes. Additionally, this research introduces two DIP-based segregation indices: one based on the distribution of aggregates in horizontally sawn sections and another focused on vertically sawn sections from hardened concrete specimens.

2. MATERIALS AND METHODS

2.1 Materials

In this study, the concrete samples were all prepared using OIVA-cement CEM II 42.5 N from Finnsementti, based in Parainen, Finland. Table 1 provides a detailed breakdown of the clinker's chemical components. Notably, OIVA cement contains between 21% and 35% added limestone and ground granulated blast-furnace slag, which has a lower climate impact and is commonly used in air-entrained concrete in Finland.

Table 1 — The chemical composition of the clinker of OIVA-cement CEM II 42.5 N

Chemical Composition	Mass percentage volume (%)
CaO	64–66
SiO_2	20–22
Al_2O_3	4.0–5.4
Fe_2O_3	2.8–3.2
MgO	2.5–3.2
SO_3	3.0–3.3

The aggregates were granitic gravel and white limestone, which all had a water absorption of 0.8%. Each mixture contained six different fraction sizes of granitic gravel and one fraction size of the white limestone, where the latter corresponded to the largest fraction size 8–16 mm. Table 2 presents the sizes and distribution of all aggregates. The specific gravities for the cement, granitic gravel, and white limestone were 3.15, 2.68, and 2.72 respectively. The mixtures composed of 430 kg/m³ of cement, 170 kg/m³ of effective water, which is the water remaining after absorption by the aggregates, and 1703 kg/m³ of aggregates. Hence, the mixtures had a water-to-cement ratio of 0.395. Additionally, the concrete was air-entrained using BASF MasterAir 100 from Finland, and the superplasticizer BASF MasterGlenium SKY 600 from Finland was used to achieve the target workability. The doses for the air-entraining agent and the superplasticizer were 0.025% and 0.77% of cement weight, respectively. This recipe was designed to produce concrete with an average air content of 6% and an S4 slump class, i.e., a slump within the range of 160–210 mm.

Table 2– Combined aggregates sizes and their weight proportions of the total aggregates in the concrete mixture

Aggregate type	Fraction (Diameter in mm)	Weight Proportion (%)	Sieve size (mm)									
			0.125	0.25	0.5	1.0	2.0	4.0	8.0	16.0	32.0	64.0
Filler	< 1	8	42	81	93	97	98	100	100	100	100	100
Fine Aggregates (FA)	0.1 – 0.6	12	3	21	76	100	100	100	100	100	100	100
	0.5 – 1.2	12	0	2	6	70	100	100	100	100	100	100
	1.0 – 2.0	15	0	1	2	7	79	100	100	100	100	100
	2.0 – 5.0	15	0	0	1	1	1	47	100	100	100	100
Coarse Aggregates (CA)	5.0 – 10.0	18	0	0	0	0	0	3	82	100	100	100
	8.0 – 16.0	20	0	0	0	0	0	0	5	99	100	100
Combined Aggregates (%)			4	9	18	29	44	55	78	100	100	100

2.2 Methods

Concrete mixing, casting, and compaction

Eight concrete batches were prepared under consistent conditions. Each batch was mixed for three minutes and 30 seconds at a controlled room temperature of 20 ± 2 °C. Immediately after mixing, several tests were conducted on the fresh concrete: the slump was measured as per SFS-EN 12350-2, the fresh density was determined following SFS-EN 12350-6 guidelines, and the air content was assessed using the pressure gauge method in accordance with SFS-EN 12350-7.

Table 3 details the specimens cast from each batch, with their labels indicating the compaction method and vibration time. Specimens labelled with a "P" prefix were compacted using the poker vibrator Wacker Neuson IRFU 30/5. This vibrator has a head that is 350 mm long and 30 mm in diameter, operating at a vibration frequency of 200 Hz, which produces an effective vibration diameter of 40 cm. The vibrator was inserted into the centre of each filled mould and was maintained at an approximate distance of 20–30 mm throughout the compaction process, and then pulled out slowly and kept vertical as much as possible.

Table 3 – Specimens from table and poker-vibrated concrete batches, T and P respectively

Batch No.	Cast specimens
1	P12 & P27
2	P16 & P30
3	P6 & P40
4	P10 & P18
5	P20 & P35
6	P6_8 & P40_8
7	T140, T120, T100 & T80
8	T60, T50 & T40

This research aims to investigate as wide of a segregation spectrum as possible, hence we used an extensive range of vibration times for both P- and T-specimens. The vibration time for P-specimens ranged from 6 to 40 seconds, with the number following the "P" indicating the specific vibration time. For instance, P12 was vibrated for 12 seconds. The compaction of P-specimens was monitored using a stopwatch. P-specimens were cast in a custom wooden mould with a Plexiglas front, measuring 200 mm in length, 200 mm in width, and 300 mm in height.

On the other hand, specimens with a "T" prefix were compacted with the High-Frequency Vibrating Table 2.0271SU, which offers an adjustable frequency range of 67 – 150 Hz. The vibration time for T-specimens spanned from 40 to 140 seconds, with the number following the "T" denoting the specific vibration time. The vibration times for T-specimens were adjusted using a timer switch built into the table, and the frequency was fixed to 150 Hz. T-specimens were cast into cylindrical metallic moulds with an inner diameter of 150 mm and a height of 300 mm.

Sawing and density measurements
After compaction, all specimens were allowed to harden in their moulds for 48 hours at room temperature (20 ± 2 °C). Subsequently, the specimens were demoulded and sawn. As illustrated in Figure 1, a 25-mm thick vertical section was sawn from the side of each specimen. The remaining part of the specimen was then divided into 10 horizontal slices, each around 25 mm thick. All sections and slices were sawn using a diamond blade saw with a blade thickness of 5 mm. The densities of the horizontal slices were determined according to SFS-EN 12390-7. For this, each slice was weighed in air and then underwater. The density was calculated by comparing the weight in air to the weight difference between the air and underwater measurements.

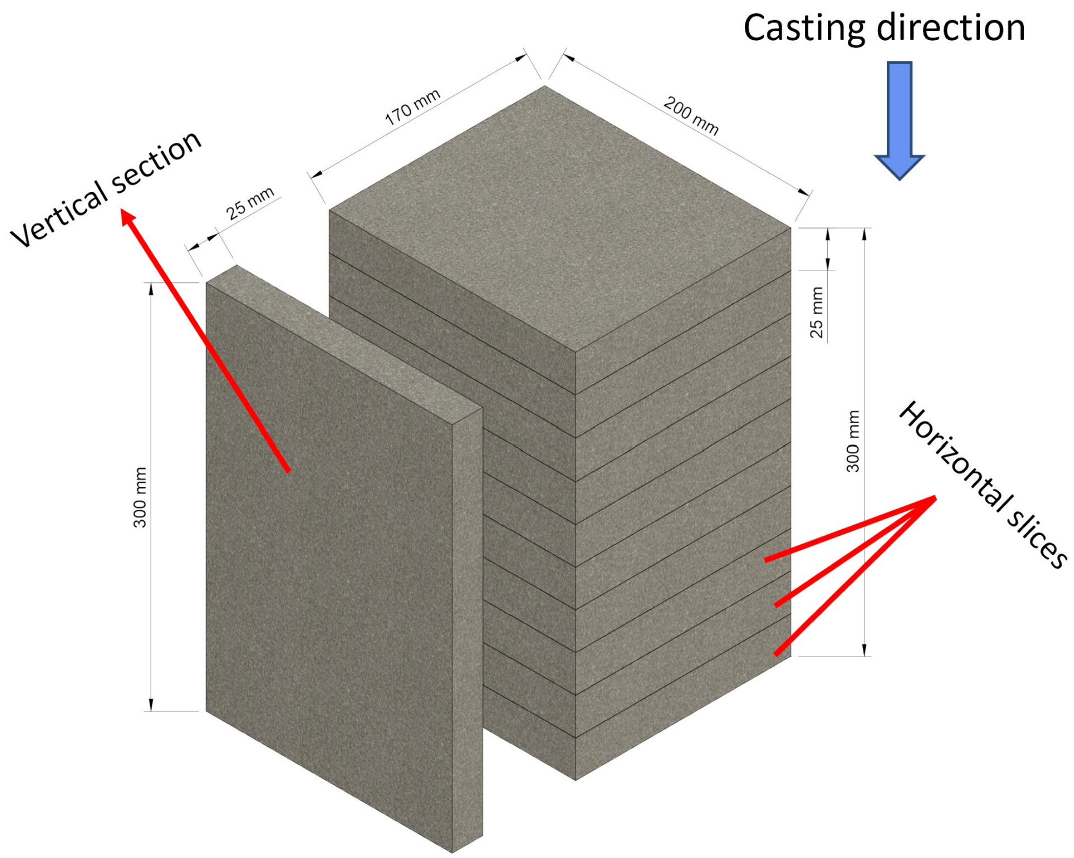

Figure 1 – Schematic representation of the sawn sections in a hardened P-specimen with the casting direction highlighted with the downwards arrow.

Digital Image Processing (DIP)

DIP is incorporated into this study as an additional method of analysis due to its efficiency and potential for future development. A key advantage of DIP lies in its ability to rapidly process data; scanning concrete slices takes approximately one minute, and multiple slices can be simultaneously scanned depending on their size. Following the scan, Python code is employed to analyze the images, with each requiring about 3 seconds for processing. This method requires less time compared to density measurements, which involve weighing of each specimen in air and water, along with the necessary wait for scale stabilization. Furthermore, the implementation of DIP using Python allows for improvements and adaptations for future research.

Five horizontal slices were selected from each specimen to be scanned with an Epson Perfection V37 flatbed scanner at a resolution of 1200 DPI. The bottom side of each odd-numbered slice was scanned, so that DIP was carried out at depths of 25 mm, 85 mm, 145 mm, 205 mm, and 265 mm from the top of the specimen. The analysed region spanned 90x140 mm² and 95x95 mm for P-specimens and T-specimens, respectively. Additionally, the vertically sawn section from each specimen underwent scanning at the same DPI. The analysed area for each vertical section of P-specimens was 190x290 mm², and for T-specimens, they measured 90x270 mm².

The image analysis described in this study was performed using Python, with key functionalities provided by several libraries including OpenCV, NumPy, SciPy, and scikit-image. Colour thresholding was employed to automatically isolate the aggregates within each image. As shown in Figure 2, three different tones of aggregates are found in each slice: white-toned, red-toned, and black-toned. It was established earlier that the largest aggregate fraction, measuring 8–16 mm, consists of white limestone, which accounts for the predominance of white-toned aggregates in this size range. In contrast, the other aggregates, primarily granitic in composition, exhibit red and black tones.

Each aggregate type was isolated using specific Hue-Saturation-Value (HSV) thresholds tailored to its colour characteristics. The ‘Hue’ component represents the colour type, such as red, blue, or green, ‘Saturation’ describes the intensity of the colour from vivid to grey, and ‘Value’ indicates the brightness of that colour. The RGB images were first converted to the HSV colour space, which is more suitable for colour-based thresholding. For instance, white-toned aggregates were detected using an HSV range of (0.004, 0.999) for hue, (0.000, 0.079) for saturation, and (0.790, 1.000) for value. Similar specific ranges were defined for red-toned and black-toned aggregates.

After thresholding, the binary masks underwent a post-processing step to isolate larger aggregates. This involved using connected components analysis to filter out regions based on their area, ensuring that only aggregates larger than 5 mm were considered. Morphological operations, specifically the closing operation, were applied to fill small holes within the detected aggregates. The final processed images represent a binary mask of the aggregates, where white pixels denote the presence of aggregates and black pixels denote the absence. The area ratio of these aggregates was then calculated to determine the percentage of each aggregate type in the scanned slice. For examples, the slice shown in Figure 2 has 8.6% white-toned aggregates, 6.0% black-toned aggregates, and 5.4% red-toned aggregates, with a total of 20% aggregates in the whole slice.

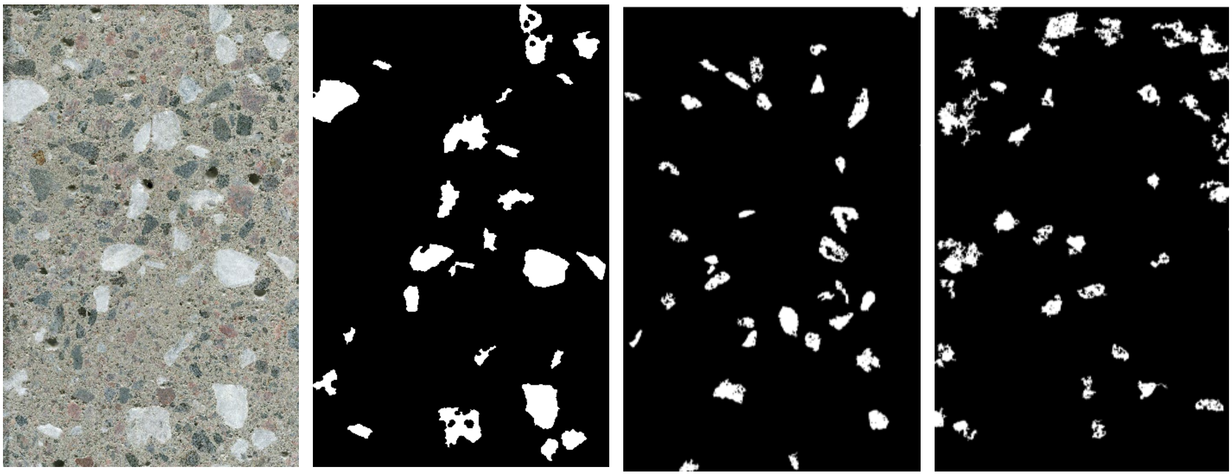

Figure 2 – Original scan of a concrete horizontal slice and its corresponding binary masks highlighting white-toned, red-toned, and black-toned aggregates larger than 5 mm.

The same DIP approach was applied to the scans of the vertical sections. In this case, an additional step was taken: the binary images representing the three aggregate types were merged into a single composite binary image. This combined image was then digitally segmented into ten equal slices, mirroring the physical horizontal slices obtained from the sawing process.

Although the DIP method employed effectively isolates the aggregates, it is worth noting some inherent challenges. Due to the natural variability in aggregate colouration, not all parts of an aggregate might be captured perfectly by the HSV limits. Specifically, the edges of many aggregates, which may have colours blending with the cement paste, might not be 100% delineated. Additionally, some aggregates may exhibit internal holes or inconsistencies that aren't always recognized as part of the aggregate by the processing algorithm.

To quantify the error in aggregate detection using the colour thresholding algorithm, a manual correction process was conducted on four different scans. Each scan was selected from a different specimen at varying depths, specifically PO2 at 25 mm, PN1 at 85 mm, PN2 at 145 mm, and PO1 at 265 mm. This selection ensured a comprehensive representation of the distributions of white-toned, red-toned, and black-toned aggregates at different depths and with different concentrations. The correction process entailed overlaying three binary images representing the different colour aggregates onto the original scans. Using the brush tool in Photoshop, the edges were refined, and any gaps were filled to accurately depict the aggregate distribution. Following this, the corrected aggregate percentages were recalculated using a similar Python script. The comparison between the originally detected and the manually corrected percentages yielded an error range from 0.1% to 0.6% across the twelve corrections, with the average error being 0.4%. Such error is unlikely to significantly alter the aggregate percentage measurements, given the scale and scope of the analysis. Thus, the method should provide a reliable and representative view of aggregate distribution within each slice.

3. RESULTS

3.1 Fresh concrete properties

All batches met the S4 concrete criteria, supporting their comparability for this study, as detailed in Table 4. The mean slump value across the batches was 186 mm ± 8 mm. Except for batch 6, the air content was also consistent, with a mean of 6.3% ± 0.5%. Batch 6 deviated with a higher air entrainment level of 8.1%. To denote this, specimens from batch 6 are labelled with an '_8' after the vibration time, such as P6_8 and P40_8.

Table 4 – Slump and air content values for the eight concrete batches

Batch No.	Slump (mm)	Air Conetnt
1	165	7.3%
2	180	6.2%
3	205	5.9%
4	195	6.0%
5	195	6.7%
6	182	8.1%
7	190	6.1%
8	178	6.1%

3.2 Density results

Density profiles using horizontal slices

The densities of the ten slices from each specimen were plotted against their respective depths to create density profiles as shown in Figures 3 and 4 for P- and T-specimens, respectively. Figure 3 illustrates these profiles for P-specimens, grouping pairs cast from the same batch into individual subplots. Similarly, density profiles for T-specimens are shown in Figure 4. The measured density values for P- and T-specimens are presented in Table A.1 and Table A.2 of Appendix A, respectively.

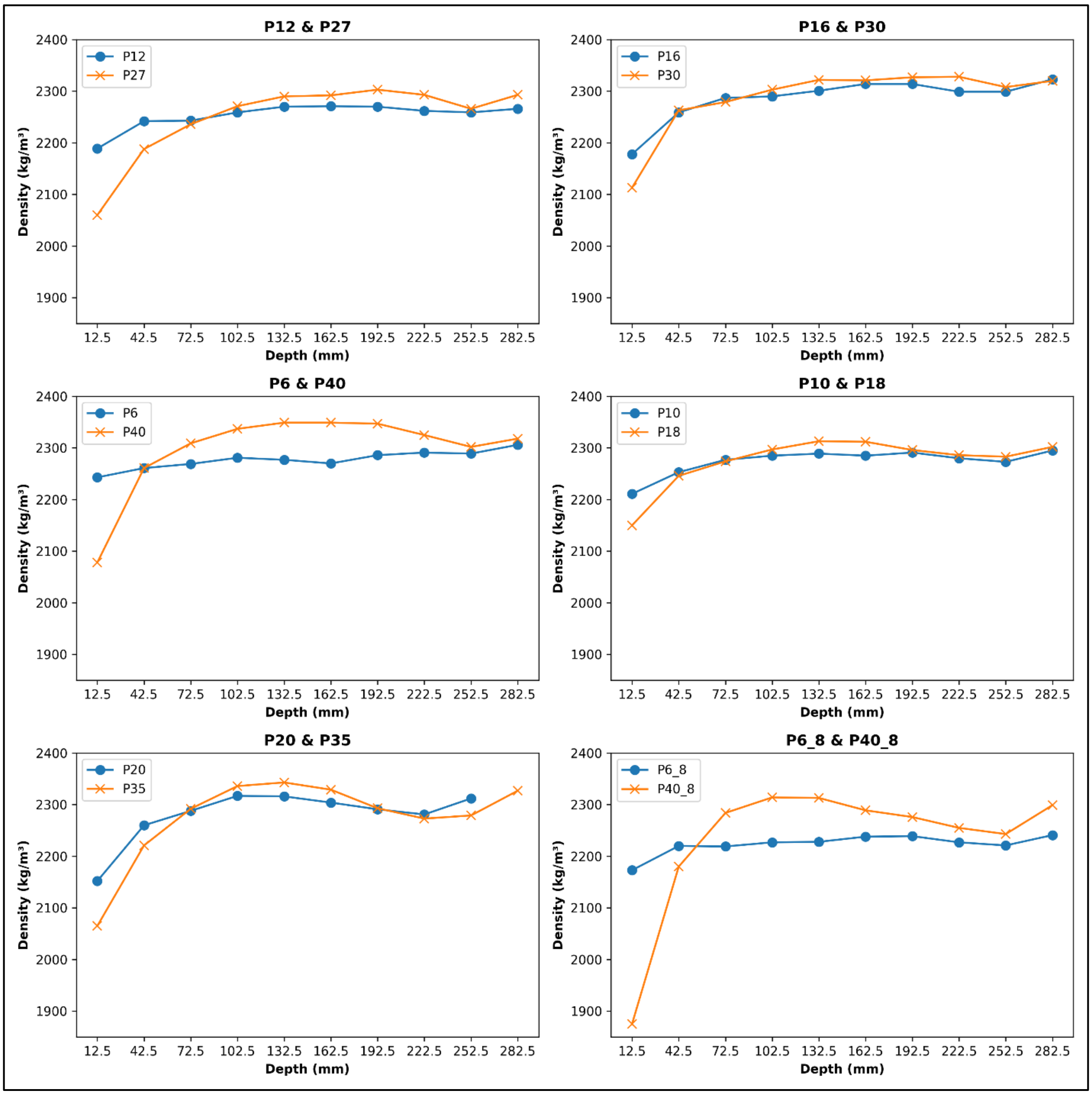

Figure 3 – Density profiles for each pair of poker-vibrated specimens (P-specimens). Note: density at 282.5 mm for P20 is missing due to a broken disc.

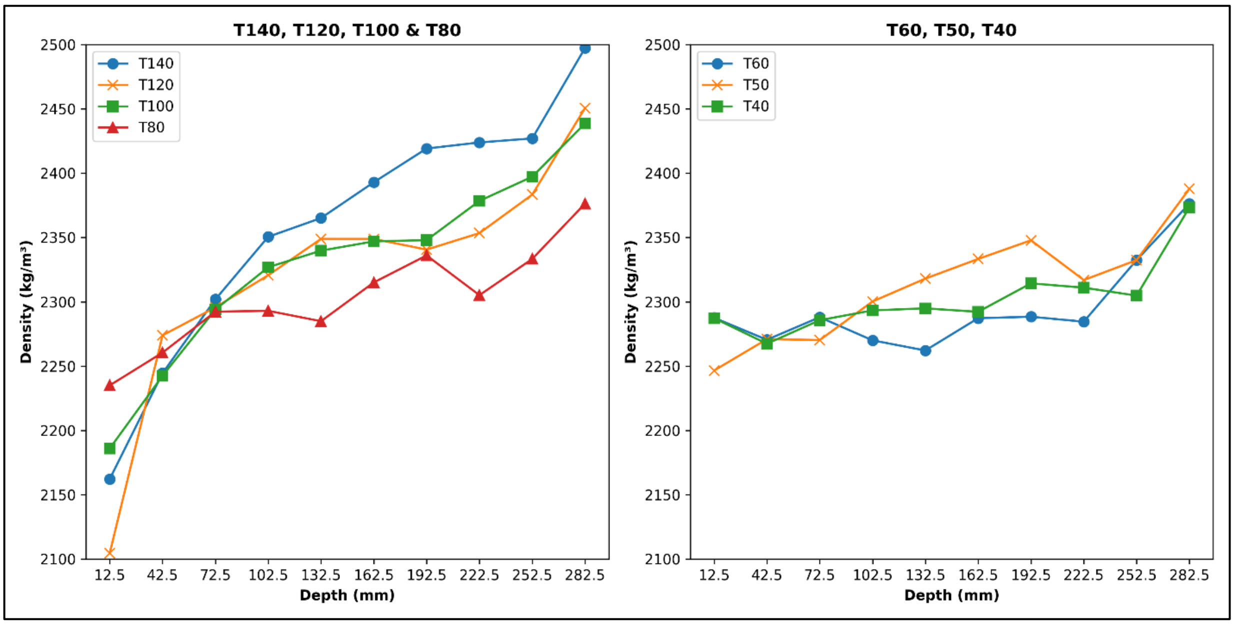

Figure 4 – Density profiles for table-vibrated specimens (T-specimens).

Segregation Index based on densities (SI_{DEN})

To assess the degree of segregation within each specimen, this study proposes a density-based segregation index, denoted as SI_{DEN}. This index is calculated as the standard deviation of the densities across the ten slices. The values for each specimen are presented in Figure 5a for P-specimens and Figure 5b for T-specimens. The classification system for the 'Segregation Level' in the legend of Figure 5 will be discussed later in the analysis and discussion chapter according to the limits specified in Table 5. SI_{DEN} is based on the inherent density differences between aggregates and cement paste. In instances of segregation, a concentration of aggregates in certain areas of the specimen would lead to variations in local density. These variations contribute to an increase in the standard deviation of densities across the slices, thereby elevating the SI_{DEN} value.

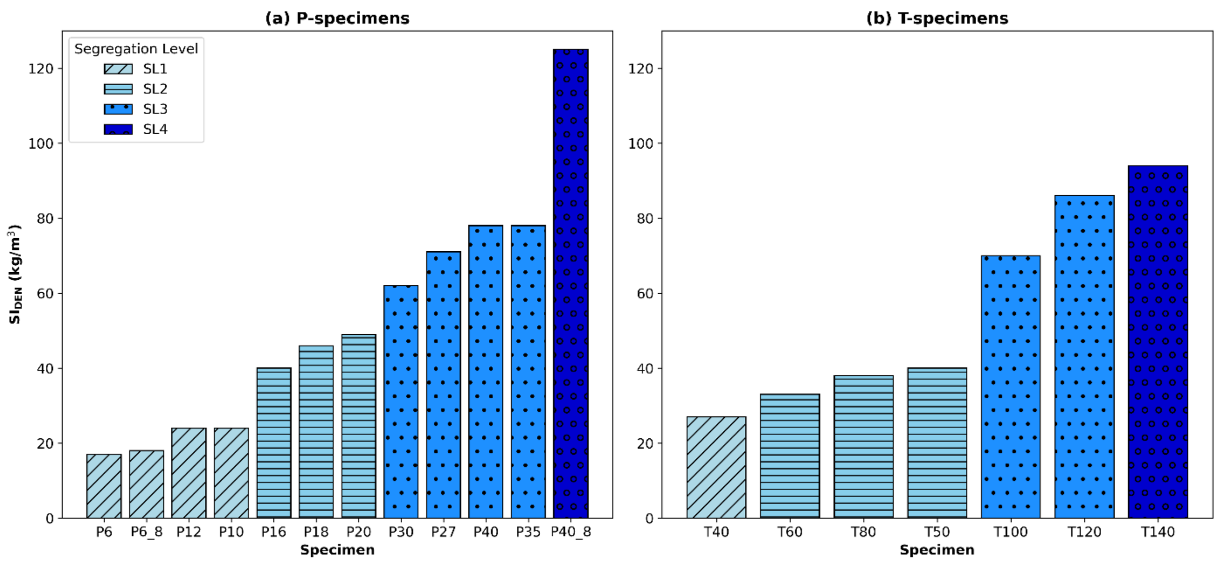

Figure 5 – Standard deviation of densities across the ten slices represented as SI_{DEN} and the corresponding segregation levels according to limits in Table 5.

Since the extent of segregation can be identified by SI_{DEN}, it is possible to specify certain limits for different levels of segregation. In this study, we propose a four-level classification system, based on which the segregation level can be either SL1, SL2, SL3, or SL4. The ranges of SI_{DEN} and their corresponding segregation levels are shown in Table 5. It is worth noting that these limits are suggestions that can be modified to align with certain applications. For instance, in watertight structures or for high load-bearing capacity elements, stricter limits could be used. More research is needed to further investigate such limits.

Table 5 – Classification of segregation levels based on SI_{DEN}

Segregation Level	Range of SI_{DEN} (kg/m³)
SL1	< 30
SL2	30–60
SL3	60–90
SL4	> 90

3.3 Digital Image Processing (DIP) results

Segregation Index based on aggregate distribution in horizontal slices (SI_{AGG_H})

To estimate the extent of segregation based on the distribution of aggregates within the specimens, this study introduces a new index, denoted as SI_{AGG_H}. This index is calculated as the standard deviation of the aggregate percentages obtained from the five horizontal slices previously discussed. The calculated SI_{AGG_H} values for each specimen are shown in Figure 6 along with their suggested segregation levels that are detailed in Table 6. The measured values for each P-specimen are shown in Table B.1 of Appendix B, and those for T-specimens are presented in Table B.2 of Appendix B.

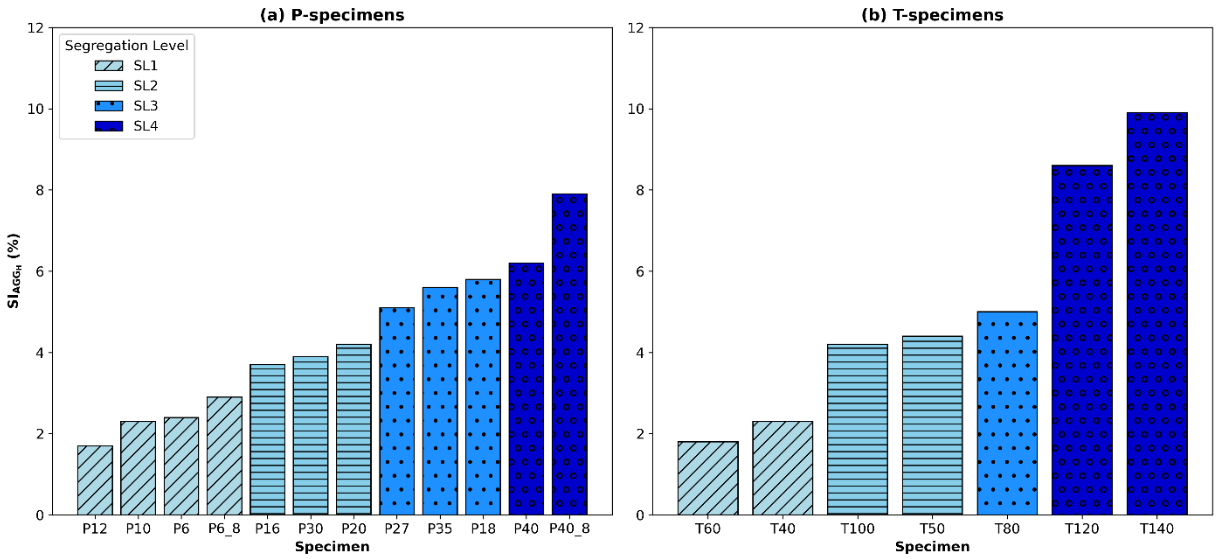

Figure 6 – Standard deviation of aggregate percentages across five slices represented as SI_{AGG_H} and the corresponding segregation levels according to limits in Table 6.

Similarly, levels of segregation can be suggested based on SI_{AGG_H} as shown in Table 6. These segregation limits were applied on our 19 specimens, and the results are illustrated with hatching patterns in Figure 6.

Table 6 – Classification of segregation levels for segregation indices based on aggregate percentages

Segregation Level	Range of SI_{AGG_H} or SI_{AGG_V}
SL1	< 3%
SL2	3% – 4.5%
SL3	4.5% – 6%
SL4	> 6%

Segregation Index based on aggregate distribution in vertical sections (SI_{AGG_V})
Another way to assess segregation is to investigate the variation of aggregates distribution within a vertical section. As previously mentioned, each vertical section was digitally divided into ten equal slices, and SI_{AGG_V} is calculated as the standard deviation of aggregate percentages across those ten slices as presented in Figure 7. The aggregate percentage within each slice for P-specimens and T-specimens are presented in Table C.1 and Table C.2 in Appendix C, respectively.

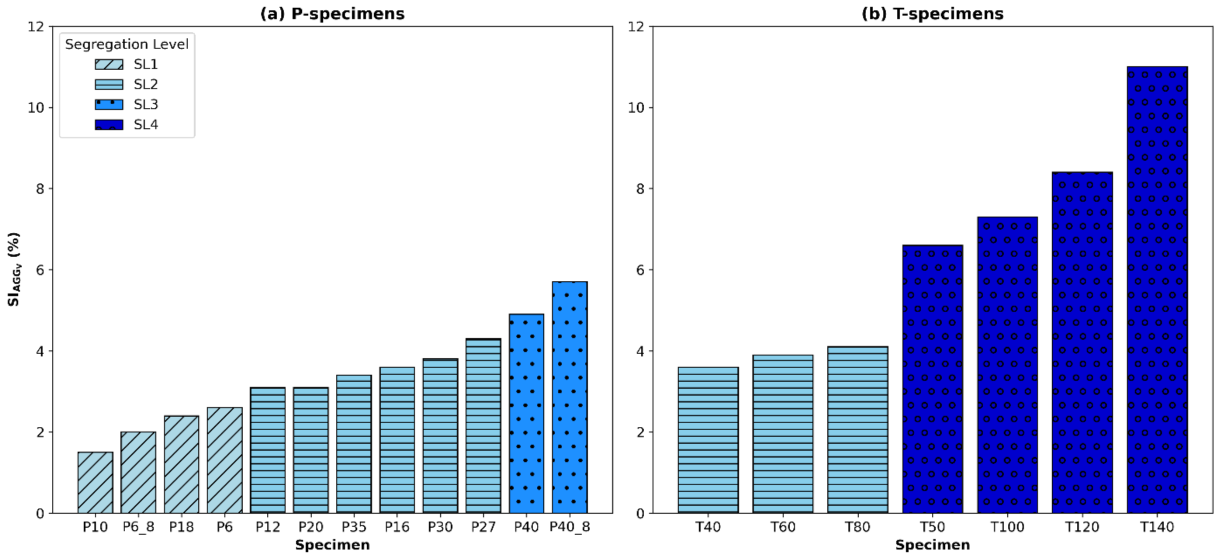

Figure 7 – Standard deviation of aggregate percentages across the ten digitally divided slices of the vertical section represented as SI_{AGG_V} and the corresponding segregation levels according to limits in Table 6.

The segregation levels suggested in Table 6 can be applied on the specimens analysed using SI_{AGG_V}, and the results are shown in Table 7 along with the segregation levels obtained via the other two indices.

Table 7 – Segregation levels for the 19 specimens based on the three different segregation indices

Specimen	Segregation level based on SI_{DEN}	Segregation Level based on SI_{AGG_H}	Segregation Level based on SI_{AGG_V}
P12	SL1	SL1	SL1
P27	SL3	SL3	SL1
P16	SL1	SL1	SL1
P30	SL3	SL1	SL1
P6	SL1	SL1	SL1
P40	SL3	SL4	SL3
P10	SL1	SL1	SL1
P18	SL1	SL3	SL1
P20	SL1	SL1	SL1
P35	SL3	SL3	SL1
P6_8	SL1	SL1	SL1
P40_8	SL4	SL4	SL3
T140	SL4	SL4	SL4
T120	SL3	SL4	SL4
T100	SL3	SL1	SL4
T80	SL1	SL3	SL1
T60	SL1	SL1	SL1
T50	SL1	SL1	SL4
T40	SL1	SL1	SL1

4. ANALYSIS AND DISCUSSION

4.1 Density analysis

Density profiles using horizontal slices

Examining Figure 3, a noticeable trend is the greater density variation in specimens subjected to longer vibration times, particularly evident in pairs with significant differences in vibration durations, such as P6 and P40. In contrast, pairs like P10 and P18 exhibit only minor variations in their density profiles.

Additionally, the most significant drop in density occurs in the top sections of the specimens, with the lowest density notably observed within the first slice, i.e., the initial 25 mm. This density drop is due to the sinking of aggregates towards the bottom as the concrete is vibrated, leaving less coarse aggregates at the top. This phenomenon is especially prevalent in P40_8, which first slice has a density of 1875 kg/m³ that is 203 kg/m³ less than its counterpart in P40. This significant drop in density for the same vibration time highlights the sensitivity of segregation relative to the air entrainment amount, as previously found by Ojala et al. [20]. Specifically, an increase in air content of 2.2% led to a 203 kg/m³ decrease in density of the uppermost part of the specimen. This higher sensitivity to segregation could be explained by the larger difference in densities between the cement paste and aggregates of an air-entrained concrete.

Interestingly, it is observed in Figure 3 that specimens P35, P40, and P40_8, which were vibrated for more than 30 seconds, show the highest densities between depths of 72.5 mm and 162.5 mm. These densities even exceed those at the bottom of the specimens. Specifically, the maximum density within this middle range is, on average, 63 kg/m³ higher than the lowest density observed at the bottom of these specimens. The reason for this density distribution might be the sinking of aggregates from the top to the middle part, but either the vibration energy or time were insufficient to segregate the aggregates all the way to the bottom.

In Figure 4, for the density profiles of T-specimens, the larger the vibration time, the more variation in density across T-specimens, similar to what is observed in P-specimens. However, for T-specimens, the density at the bottom part is always larger than that at smaller depths, which can be explained by a constant sinking of aggregates from the top towards the very bottom during vibration. Additionally, the density of the bottom slice in each specimen is higher than those of the remaining upper slices, unlike the increase of densities in the middle part observed in some P-specimens. This shows the difference in the segregation behaviour of concrete when vibrated using different methods.

Segregation Index based on densities (SI_{DEN})
As shown in Figure 5, higher SI_{DEN} values indicate greater levels of segregation. For example, the SI_{DEN} values for P16, P18, and P27 are 40 kg/m³, 46 kg/m³, and 71 kg/m³, respectively. Given that P16 and P18 were vibrated for similar durations, their SI_{DEN} values are correspondingly close. In contrast, P27, which was vibrated for a longer period, exhibits a higher SI_{DEN} value. A similar trend is observed for T-specimens, where SI_{DEN} increases with longer vibration times.

Statistical analysis revealed a strong correlation between vibration time and SI_{DEN}. For P-specimens, the correlation coefficient is $R^2 = 0.875$ and $p = 0.001$, and for T-specimens, it is $R^2 = 0.921$ and $p < 0.001$. These results suggest that SI_{DEN} serves as a reliable indicator for estimating the extent of segregation in concrete.

In setting the proposed limits shown in Table 5 for the SI_{DEN}, we considered the absence of established benchmarks within the field, necessitating an innovative approach based on empirical evidence and theoretical understanding. To capture as comprehensively as possible the segregation behaviour spectrum of this concrete, we purposefully utilized a very wide range of vibration times, as previously mentioned.

For instance, the SL1 level of segregation, with a maximum SI_{DEN} of 30 kg/m³, is characterized by relatively small fluctuations in the density of the horizontal slices. Specifically, specimen P12, which falls into the SL1 segregation class, exhibits a SI_{DEN} of 24 kg/m³, showcasing minimal density variation with the maximum difference being 82 kg/m³. Conversely, when examining SL2, and looking at specimen P20 with a SI_{DEN} of 49 kg/m³, the maximum difference in density almost doubles to 163 kg/m³. For an extreme example, specimen T140, classified under SL4, surpassed the SI_{DEN} threshold of 90 kg/m³ with a SI_{DEN} of 92 kg/m³. The variation among the discs in T140 was nearly four times that observed in P12, with the maximum density difference reaching 335 kg/m³, spanning from a minimum density of 2162 kg/m³ to a maximum of 2497 kg/m³.

It is, however, important to emphasize that these proposed limits serve as a preliminary guideline and have been suggested specifically for this concrete mix. They represent an initial step towards developing a more nuanced understanding of concrete segregation, encouraging further research to specify ranges for different mixes under varied applications.

Hence, the segregation levels, presented in Table 5, can be applied on both T- and P-specimens, as illustrated with hatching patterns in Figure 5. For T-specimens, a vibration time of 30 seconds or less typically results in an SL1 segregation, while a duration between 50 and 80 seconds leads to SL2. SL3 segregation is observed when the vibration time ranges from 100 to 120 seconds, and SL4 segregation is achieved at 140 seconds or more.

Similarly, for P-specimens, SL1 is generally observed with vibration times ranging from 6 to 12 seconds. SL2 is achieved between 16 and 20 seconds, and SL3 segregation is noted for vibration durations of 27 to 40 seconds. It is noteworthy that P40_8, which had a higher air content, exhibited a significantly higher SI_{DEN} value of 125 kg/m³ compared to its counterpart P40, with a SI_{DEN} value of 78 kg/m³. This difference in SI_{DEN} values is reflected in their respective segregation levels, with P40 classified as 'SL3' and P40_8 as 'SL4'.

Because SI_{DEN} is based on slice densities rather than just vibration time, it allows for comparisons between different concrete mixes. For example, even though both P40 and P40_8 were vibrated for the same duration, their differing SI_{DEN} values reveal distinct levels of segregation. This flexibility extends to comparing mixes vibrated using different methods. For example, T50 and P16, despite different vibration methods and durations, have identical SI_{DEN} values, indicating a similar extent of segregation. This makes SI_{DEN} a versatile tool for assessing segregation across a variety of conditions.

4.2 DIP analysis

Segregation Index based on aggregate distribution in horizontal slices (SI_{AGG_H})
To assess the effectiveness of SI_{AGG_H}, presented in Figure 6, its correlation with SI_{DEN} was examined. For P-specimens, the correlation was strong, with a coefficient of $R^2 = 0.846$ and $p < 0.001$. Similarly, T-specimens showed a strong correlation, with a coefficient of $R^2 = 0.891$ and $p = 0.0014$. When combining both P- and T-specimens, the correlation remained robust $R^2 = 0.839$ and $p < 0.001$. These results suggest that SI_{AGG_H}, which is based on the aggregate distribution in five slices, can be as effective as SI_{DEN}, which relies on the standard deviation of densities across ten slices, in evaluating the extent of segregation.

Comparing the SI_{AGG_H}-based segregation levels, shown in Figure 6, with those obtained using SI_{DEN}, a high degree of similarity is evident. Exceptions exist for seven out of the 19 specimens: P30, P40, P20, T120, T100, T80, and T60. It is worth noting that the discrepancies for these seven specimens are minor, differing by only one level of segregation. For instance, P30 is classified as SL2 based on SI_{AGG_H} and SL3 according to SI_{DEN}. On the other hand, P40 is considered SL4 based on SI_{AGG_H} and only SL3 according to SI_{DEN}. Given the strong correlation and minor discrepancies between the two indices, SI_{AGG_H} proves to be a reliable alternative to SI_{DEN} for assessing the extent of segregation in concrete specimens.

Segregation Index based on aggregate distribution in vertical sections (SI_{AGG_V})
Building on our previous approach, we also investigated the correlation between SI_{AGG_V} and SI_{DEN} to gauge the effectiveness of this new index. For P-specimens, the correlation was strong, with a coefficient of $R^2 = 0.758$ and $p < 0.001$. Similarly, T-specimens also showed a strong correlation, with a coefficient $R^2 = 0.876$ and $p = 0.0019$. This proves that for each group of specimens, the sole reliance on aggregate distribution within the vertical section can successfully estimate the level of segregation.

However, when investigating the correlation for both T- and P-specimens combined, it is found that the coefficient $R^2 = 0.425$ and $p = 0.0025$. The lower combined correlation for SI_{AGG_V} may be attributed to its reliance on a single vertical slice, which may not capture the full complexity of aggregate distribution as effectively as multiple horizontal slices in SI_{AGG_H}. Additionally, the different vibration methods used for P- and T-specimens could have varying effects on vertical slices, thereby affecting the correlation of SI_{AGG_V} when both specimen types are considered together. Further investigation is needed to fully understand these discrepancies.

While SI_{AGG_V} offers the advantage of being a quicker method, requiring only the image of a single sawn section, its results may not be as easily generalizable. For instance, different compaction methods could necessitate following new segregation limits specific to those conditions. This is reflected in our results, as for P-specimens, SI_{AGG_V} ranges from 1.5% to 5.7%, whereas for T-specimens, SI_{AGG_V} ranges from 3.6% up to 11%.

As shown in Table 7, a noticeable consistency exists in the segregation levels classified by the three indices. For twelve out of 19 specimens, the segregation levels obtained by SI_{AGG_H} were the same as those acquired based on SI_{DEN}. However, the segregation levels of nine specimens were classified as the same based on SI_{AGG_V} compared to those obtained by SI_{DEN}. These specimens are P16, P6, P40, P10, P20, P6_8, T140, T80, and T60. Nine of the ten remaining specimens were classified as either one segregation level higher or lower, and the only exception is for T50, which was classified as SL4 based on SI_{AGG_V}, while its segregation level is SL1 based on SI_{DEN}.

Similarly, there are no major differences between the segregation levels obtained by SI_{AGG_H} and SI_{AGG_V} for any of the samples except for T50. Otherwise, eight specimens have the same segregation level, and the remaining ten are either one level higher or lower. These small differences highlight the unique aspects each index measures. Specifically, SI_{DEN} captures the overall density distribution, considering both possible air and aggregate segregation. SI_{AGG_H} focuses on the distribution of aggregates across multiple horizontal slices within the specimen, while SI_{AGG_V} provides insights based on a single vertical slice sawn from the side. Therefore, each index offers a slightly different but reliable approach to evaluating concrete segregation.

An important consideration in interpreting the results of our segregation indices is the inherent variability present in concrete as a composite material. Natural variations in the distribution and size of aggregates can influence the segregation indices, potentially independent of the compaction methods or durations studied here.

4.3 General discussion

This study investigates segregation within similar concrete mixes that are vibrated for different durations using two different methods: poker and table vibrators. Three segregation indices are proposed: SI_{DEN}, SI_{AGG_H}, and SI_{AGG_V}. While SI_{DEN} considers both the effects of aggregate and air segregation, it requires the longest preparation time, as the specimen must be sawn into 10 horizontal slices, and each should be weighed in air and under water. On the other hand, SI_{AGG_H} shortens the preparation time, as it requires the images of five slices only. Whereas SI_{AGG_V} requires the least time, as it can be calculated from the image of one sawn vertical section, and it correlates highly with SI_{DEN}.

It is possible to estimate the segregation sensitivity of a mix based on the average rate of change of one of the segregation indices. For example, if we consider T-specimens only, the average rate of change of SI_{DEN} is 0.6 kg/m^3 per second of vibration. This rate of change can be compared to those of other mixes vibrated by the same table at the same frequency, and the higher the rate of change, the more sensitive that mix is to segregation. Another possibility to estimate segregation sensitivity is to calculate the difference between maximum and minimum values of a certain index. For instance, the range of SI_{AGG_H} for our mix is 8.2%. In case we had another mix which range of SI_{AGG_H} is 16%, then we can say that the second mix is almost two times more sensitive to segregation than our mix.

It is important to note some limitations when applying the proposed segregation indices to cores drilled from existing structures. One key limitation is the direction of drilling; this research assumes cores are drilled vertically to obtain a vertical distribution of either densities or aggregate percentages. Another consideration is the casting layer. The specimens analysed in this study represent a single casting layer, but cores from existing structures may include multiple compacted layers. However, if information on the casting layers is available and vertical drilling is assured, the proposed segregation indices can assess segregation levels in existing structures.

There are several avenues for future research. The primary focus could be on testing different concrete mixtures to establish more comprehensive limits for segregation levels and to investigate the segregation sensitivity of various mixes. Additionally, software could be developed to implement the colour-thresholding algorithm on smartphones, enabling an instant calculation of SI_{AGG_V} after sawing a single vertical section after adjusting the colour-thresholds based on the colours of aggregates. Furthermore, the algorithm for aggregate detection could also be enhanced using deep learning approaches, which can eliminate the need for setting certain colour-thresholds for each concrete.

5. CONCLUSIONS

In concrete compaction, segregation is a critical issue that affects both durability and structural performance. This study introduced and evaluated three distinct segregation indices to assess the extent of segregation in concretes cast using the same recipe. These indices were applied to two sets of specimens: those vibrated using a poker vibrator (P-specimens) and those using a table vibrator (T-specimens), each subjected to varying durations of vibration. The first index is based on the distribution of density within the specimen, while the other two indices focus on the spatial distribution of aggregates. Specifically, one of these latter indices utilizes multiple horizontal slices, and the other employs a single vertical slice, both acquired through DIP. Importantly, these indices have the potential to be applied in evaluating segregation in cores drilled from existing structures, as well as in testing the sensitivity of new concrete mixes to segregation induced by different compaction methods and or times. The following conclusions are drawn based on these assessments.

- The distribution of densities within a specimen represents the extent of segregation of that specimen. This is achieved by calculating the standard deviation of densities of ten horizontally sawn slices from each specimen, noted as SI_{DEN}. It was found that SI_{DEN} highly correlates with the vibration time, such that the correlation coefficients are 0.875 and 0.921 for P-specimens and T-specimens, respectively.
- The distribution of aggregates larger than 5 mm within a specimen can be used as an alternative to density distribution to assess segregation. This is reflected in the use of SI_{AGG_H} that relies on the standard deviation of aggregate percentages in five horizontal slices from one specimen. SI_{AGG_H} shows a high correlation of 0.839 with SI_{DEN} regardless of the vibration method.

- The most time-efficient approach involves analysing the distribution of aggregates within a single vertical slice. The obtained index, referred to as SI_{AGG_V}, correlates well with SI_{DEN}, as their correlation coefficients are 0.758 and 0.876 for P-specimens and T-specimens, respectively.
- Based on either of the segregation indices, segregation levels can be proposed. In this article, four segregation levels were suggested; SL1, SL2, SL3, and SL4. The limits for these levels can vary based on the expected structural performance of the tested concrete.
- An increase in air entrainment from approximately 6.5% to 8% led to a significant rise in all three segregation indices. This suggests the potential impact of increased air entrainment on the segregation behaviour of the studied concrete mix. Further research is needed to fully understand the extent and nature of this influence.

REFERENCES

1. Yan W, Cui W, Qi L: "Effect of Aggregate Gradation and Mortar Rheology on Static Segregation of Self-Compacting Concrete". *Construction and Building Materials*, Vol., No. 259, 2020.
2. Cui W, Miao RC, Yan WS, Song H, Jiang Z: "Static Segregation of Fresh High Workable Concrete Based on an Image Processing Method". *Construction and Building Materials*, Vol. 361, No. 129708, 2022.
3. Neville AM: "Properties of Concrete 5th ed.". Chapter 4, “Fresh Concrete”. Pearson, Harlow, England; New York, USA, 2011.
4. Mehta PK, Monteiro PJM: "Concrete Microstructure, Properties, and Materials”, 3rd ed., McGraw-Hill Professional Publishing, 2005, pp. 362-453.
5. Breul P, Geoffray J-M, Haddani Y: "On-Site Concrete Segregation Estimation Using Image Analysis". *Journal of Advanced Concrete Technology*, Vol. 6, No. 1, 2008, pp. 171-180.
6. Navarrete I, Lopez M: "Estimating the Segregation of Concrete Based on Mixture Design and Vibratory Energy". *Construction and Building Materials*, Vol. 122, , 2016, pp. 384-390.
7. Solak AM, Tenza-Abril AJ, Baeza-Brotons F: "Image Analysis Applications for the Study of Segregation in Lightweight Concretes". *International Journal of Computational Methods and Experimental Measurements*, Vol. 6, No. 4, 2018, pp. 835-846.
8. Ozen M, Guler M: "Quantification of Segregation in Portland Cement Concrete Based on Spatial Distribution of Aggregate Size Fractions". *Image Analysis and Stereology,* Vol. 39, 2020.
9. Ojala T, Ahmed H, Kuusela P, Seppänen A, Punkki J: "Monitoring of Concrete Segregation Using AC Impedance Spectroscopy". *Construction and Building Materials*, Vol. 384, No. 131453, 2023.
10. American Concrete Institute Committee 309: "Guide for Consolidation of Concrete". 2005.
11. Cement Concrete and Aggregates Australia: "Compaction of Concrete". 2006.
12. Khayat KH: "Use of Viscosity-Modifying Admixture to Enhance Stability of Fluid Concrete". *ACI Materials Journal,* Vol. 94, No. 4, 1997, pp. 332-340.
13. Safawi MI, Iwaki I, Miura T: "The Segregation Tendency in the Vibration of High Fluidity Concrete". *Cement and Concrete Research*, Vol. 34, No. 2, 2004, pp. 219-226.
14. Yu QL, Spiesz P, Brouwers HJH: "Ultra-Lightweight Concrete: Conceptual Design and Performance Evaluation". *Cement and Concrete Composites*, Vol. 61, , 2015, pp. 18-28.

15. Yim HJ, Bae YH, Kim JH: "Method for Evaluating Segregation in Self-Consolidating Concrete Using Electrical Resistivity Measurements". *Construction and Building Materials*, Vol. 19, 2023.
16. Barbosa FS, Beaucour AL, Farage MCR, Ortola S: "Image Processing Applied to the Analysis of Segregation in Lightweight Aggregate Concretes". *Construction and Building Materials*, Vol. 25, 2011, pp. 3375-3381.
17. Ke Y, Beaucour AL, Ortola S, Dumontet H, Cabrillac R: "Influence of Volume Fraction and Characteristics of Lightweight Aggregates on the Mechanical Properties of Concrete". *Construction and Building Materials*, Vol. 23, 2009, pp. 2821-2828.
18. Mesbah HA, Yahia A, Khayat KH: "Electrical Conductivity Method to Assess Static Stability of Self-Consolidating Concrete". *Cement and Concrete Research*, Vol. 41, 2011, pp. 451-458.
19. Nili M, Razmara M, Nili M, Razmara P: "Proposing New Methods to Appraise Segregation Resistance of Self-Consolidating Concrete Based on Electrical Resistivity". *Construction and Building Materials*, Vol. 146, 2017, pp. 192-198.
20. Ojala T, Al-Neshawy F, Punkki J: "Effect of Concrete Composition on its Compactability" ("Betonin koostumuksen vaikutus sen tiivistettävyyteen"). *Report on a commissioned research project.* Aalto University, Department of Civil Engineering, Espoo, Finland, 2019. (In Finnish)
21. Westendarp A: "Concrete Mix Stability Problems" ("Probleme mit der Mischungsstabilität von Beton"). *BAWBrief.* Hydraulic Engineering Repository, Germany, 2015. (In German)

APPENDIX A

Table A.1 – Measured disc density values for poker-vibrated specimens (P-specimens)

Depth (mm)	P12	P27	P16	P30	P6	P40	P10	P18	P20	P35	P6_8	P40_8
	Density (kg/m³)											
12.5	2189	2060	2178	2113	2243	2078	2211	2150	2152	2065	2173	1875
42.5	2242	2188	2259	2263	2261	2261	2253	2246	2260	2221	2220	2180
72.5	2243	2236	2287	2279	2269	2309	2277	2274	2288	2292	2219	2284
102.5	2259	2271	2290	2303	2281	2337	2285	2297	2317	2336	2227	2314
132.5	2270	2290	2301	2322	2277	2349	2289	2313	2316	2343	2228	2313
162.5	2271	2292	2314	2321	2270	2349	2285	2312	2304	2329	2238	2289
192.5	2270	2303	2314	2327	2286	2347	2291	2296	2291	2293	2239	2276
222.5	2262	2293	2299	2328	2291	2325	2280	2286	2281	2273	2227	2255
252.5	2259	2266	2299	2308	2289	2302	2273	2283	2312	2279	2221	2243
282.5	2266	2293	2323	2320	2306	2318	2295	2302	—	2327	2241	2299

Table A.2 – Measured disc density values for table-vibrated specimens (T-specimens)

Depth (mm)	T140	T120	T100	T80	T60	T50	T40
	Density (kg/m³)						
12.5	2162	2105	2186	2235	2288	2247	2287
42.5	2245	2274	2243	2261	2270	2271	2267
72.5	2302	2296	2294	2292	2288	2270	2286
102.5	2351	2321	2327	2293	2270	2300	2293
132.5	2365	2349	2340	2285	2262	2318	2295
162.5	2393	2349	2347	2315	2287	2333	2292
192.5	2419	2341	2348	2336	2288	2348	2314
222.5	2424	2353	2378	2305	2285	2317	2311
252.5	2427	2383	2397	2333	2332	2332	2305
282.5	2497	2451	2439	2376	2376	2388	2373

APPENDIX B

Table B.1 – Calculated aggregate percentage distributions from the five horizontal slices of poker-vibrated specimens (P-specimens)

Depth (mm)	P12	P27	P16	P30	P6	P40	P10	P18	P20	P35	P6_8	P40_8
	Aggregate percentage (%)											
25	15	3	12	7	16	10	15	7	15	6	17	2
85	16	14	20	25	19	19	21	19	14	18	17	23
145	18	19	23	17	20	25	23	24	23	27	18	30
205	17	19	19	25	23	28	19	28	22	24	22	28
265	19	27	25	20	23	26	20	22	21	23	21	26

Table B.2 – Calculated aggregate percentage distributions from the five horizontal slices of table-vibrated specimens (T-specimens)

Depth (mm)	T140	T120	T100	T80	T60	T50	T40
	Aggregate percentage (%)						
25	20	7	9	13	18	15	18
85	16	22	16	22	16	18	16
145	31	27	21	26	17	23	17
205	29	29	26	19	21	24	18
265	31	34	19	23	22	23	21

APPENDIX C

Table C.1 – Calculated aggregate percentage distributions from the vertical slice of poker-vibrated specimens (P-specimens)

Depth (mm)	P12	P27	P16	P30	P6	P40	P10	P18	P20	P35	P6_8	P40_8
	Aggregate percentage (%)											
12.5	11	13	14	14	19	8	18	10	14	13	16	3
42.5	14	16	16	14	19	16	18	17	18	16	21	13
72.5	15	19	15	27	12	26	15	18	23	17	15	24
102.5	14	20	20	23	13	22	14	17	22	24	18	18
132.5	20	18	15	22	14	19	18	16	17	24	20	16
162.5	19	24	21	21	15	25	14	19	21	19	20	17
192.5	18	17	14	22	16	15	16	15	23	17	16	16
222.5	25	17	20	21	21	19	16	16	22	19	15	19
252.5	13	17	19	20	23	18	16	17	19	22	18	20
282.5	24	22	17	19	20	21	17	18	25	17	16	24

Table C.1 – Calculated aggregate percentage distributions from the vertical slice of table-vibrated specimens (T-specimens)

Depth (mm)	T140	T120	T100	T80	T60	T50	T40
	Aggregate percentage (%)						
12.5	4	2	16	5	16	7	16
42.5	3	5	16	9	17	11	9
72.5	4	20	16	10	17	14	11
102.5	14	14	15	16	20	11	16
132.5	21	16	19	16	12	16	12
162.5	23	21	10	29	25	24	11
192.5	28	18	14	19	15	16	7
222.5	34	10	20	21	15	19	18
252.5	23	20	26	24	20	23	7
282.5	29	33	15	25	14	30	17